Implementation of sonicated continuous plug flow crystallization technology for processing of acetylsalicylic acid reaction mixture

Kornélia Tacsi [a], György Stoffán [a], Éva Pusztai [b], Brigitta Nagy [a], András Domokos [a], Botond Szilágyi [c], Zsombor Kristóf Nagy [a], György Marosi [a,*], Hajnalka Pataki [a,*]

[a] Department of Organic Chemistry and Technology, Faculty of Chemical Technology and Biotechnology, Budapest University of Technology and Economics, Műegyetem rkp. 3., H-1111 Budapest, Hungary
[b] Department of Chemical and Environmental Process Engineering, Faculty of Chemical Technology and Biotechnology, Budapest University of Technology and Economics, Műegyetem rkp. 3., H-1111 Budapest, Hungary
[c] Faculty of Chemical Technology and Biotechnology, Budapest University of Technology and Economics, Műegyetem rkp. 3., H-1111 Budapest, Hungary

ARTICLE INFO

ABSTRACT

An effective way to ensure proper mixing and thereby realize maintenance-free operation of the clogging-sensitive continuous tubular crystallizers is the utilization of ultrasound-irradiation. Considering this, our research aimed to develop an ultrasonicated plug flow crystallization process to separate and purify a multicomponent acetylsalicylic acid (ASA) flow reaction mixture with antisolvent and combined cooling-antisolvent method. The influence of process parameters – temperature, antisolvent to ASA solution ratio, mean residence time – on purity, yield, productivity, product size, and size distribution was investigated applying a 2^3 full factorial experimental design. In further analysis, the alteration of product quality and quantity was studied by reducing the ultrasonicated tubing length and increasing the feeding rate, which could be important for industrial applicability. It was found that ultrasonication results in robustness against process parameter modification regarding product quality producing purified, small (<50 μm), consistent quality product while enabling to reach 89% yield even with 30 s residence time.

© 2022 Published by Elsevier B.V.

1. Introduction

In recent decades, driven by the need for more economical and efficient production in the pharmaceutical industry, the regulatory authorities in cooperation with the pharmaceutical companies have encouraged the conversion from batch to continuous processes. Based on this paradigm shift, continuous crystallization was soon the subject of increased attention due to its process robustness and high productivity. The traditionally applied batch crystallization has issues with batch-to-batch variations in product quality [1]. In contrast, a continuous crystallizer under steady-state conditions produces a solid product with lower quality fluctuations [2].

Continuous crystallization systems can be divided into two major groups: mixed suspension mixed product removal (MSMPR) crystallizers and continuous tubular crystallizers [3]. The MSMPR crystallizer setups are similar to the stirred tank reactors [4–8] and are usually used for crystallization systems with slower kinetics requiring longer residence time (RT). The tubular crystallizers preferably promote the fed components to flow at a constant velocity and as homogeneous slurry.

The various types of continuous tubular crystallizers are the plug flow crystallizer (PFC) [9], the continuous oscillatory baffled crystallizers (COBCs) [10], and the continuous segmented flow crystallizers (CSFCs) [11–14]. The use of tubular crystallizers is beneficial for their high efficiency in terms of yield [15], narrower RT distribution, and easier scale-up. The drawbacks of these systems are their complicated and expensive maintenance and relatively high development demand [2]. Furthermore, the fouling and particle deposition could easily cause plugging complications, especially in the case of narrow tubular reactors [16,17].

Efficient mixing is essential, especially when high supersaturation is present at the mixing region where the solution of the active pharmaceutical ingredient (API) is blended with the stream of an antisolvent [18] or a reactant [19,20]. For this purpose, several mixing elements were developed, such as T-mixers [1], Y-mixers [21–23], Roughton type mixers [4,24,25], radial [26], and also coaxial mixers [27–30]. The use of Y-mixers – and also T-mixers – is limited as their mixing efficiency is lower compared to Roughton type or two jet vortex mixers

---

* Corresponding authors.
E-mail addresses: marosi.gyorgy@vbk.bme.hu (G. Marosi), pataki.hajnalka@vbk.bme.hu (H. Pataki).

[25], especially at different feed rates. The mixing of streams with unequal volumetric flow rates could also be performed using a coaxial mixer (co-flow or concentric capillary mixers) [27]. Despite the benefits of coaxial mixers, its use in continuous tubular crystallizers is underrepresented, while it is widely used in flow chemistry for mixing liquid streams homogenously [31–33].

The adequate mixing of the transferred slurry in the narrow tubular crystallizer tubings is also crucial for avoiding the blockage of the equipment. The mixing of this pipe section could be ensured by static mixers [34], segmented flow [35], microwave [36], or ultrasound (US) irradiation [37]. The US can enhance crystallization by the induced cavitation that could facilitate primary nucleation, control nucleation rate, decrease induction time and metastable zone-width, affect polymorph selectivity, reduce product size and result in narrow crystal size distribution (CSD) [38,39]. The frequency, intensity, and duration of ultrasonic irradiation, the geometrical characteristics of the ultrasonic device, or even the volume of sonicated solution can affect the morphology of the product. While low-frequency US irradiation (< 100 kHz) significantly increases the rate of nucleation, the possibility of secondary nucleation and fragmentation, the effect of US on crystal growth is less significant [40]. Sonication could replace the conventional seeding method [41–43], which could be difficult to implement in continuous operation due to the requirement of accurate suspension transfer. Moreover, US irradiation aids in preventing clogging issues, ensuring the robustness of the technology. The crystal size reducing effect of the US is especially useful for poorly soluble APIs. Since, by reducing particle size the specific particle surface increases; and thus, the dissolution rate increases and the bioavailability of the drug product improves as well [44–47].

Several examples are listed in the literature about US-assisted continuous crystallizers, namely sonocrystallization in MSMPR crystallizers [48,49], COBCs [50], and PFCs. Some continuous tubular crystallizations were performed using ASA as a model active ingredient in PFC [21,22,51–55] and CSFC [12,56,57]; however, in these works, the clear ethanol solution of arbitrary ASA concentration was processed, and supersaturation was induced with cooling or water antisolvent. Some further examples utilized localized sonication for seed generation in cooling crystallization [52,56], while in other studies, the entire tubing was placed into the sonication bath to perform antisolvent [1,53,54,58] or pH swing [59] crystallizations. Hussain and co-workers developed [54] the seedless, continuous, sonicated antisolvent crystallization of ASA using a flow reactor. The ultrasonication power, initial concentration, and thereby supersaturation level was also investigated, however, the effect of temperature was not studied in a broader range. In this work, the purification efficacy of the technology was not examined, and the achieved maximum yield was ~40%. However, supersaturation was found not to affect particle size since the size and number of the cavitation bubble determine the product size predominantly.

There are further studies where the continuous acetylation of acetic acid onto salicylic acid is connected with the continuous separation and purification of the product in COBC [60] or tubular crystallizer [61]. These studies focused on either establishing an effective cleaning technique of the continuous reactor for the change between different APIs production or investigating the effect of flow rate (residence time) and nucleation temperature on crystal habit and purity. However, the effect of process parameters on purity, yield, crystal habit, size, CSD, or the long-term operability of the system was not investigated together.

In this work, we present the development of an antisolvent and combined cooling/antisolvent continuous, seedless crystallization technology for the direct procession of a complex, multi-component ASA reaction mixture using an ultrasonicated PFC system. The main aims were to produce purified small crystals with narrow CSD by developing robust manufacturing technology. Three series of experiments are performed to investigate the effect of (1) operation temperature, RT, flow rate, and antisolvent to ASA solution ratio; (2) the length of the sonicated tubing section, (3) the increase of total flow rate (TFR) on

purity, yield, crystal size, and CSD. By broadening the available CSD range of the processing, the present work provides an alternative to the continuous crystallizations previously developed by the authors for the procession of the ASA reaction mixture [62,63]. This way, a possibility of combining this technology with flow synthesis and further continuous formulation steps is presented.

2. Experimental materials and methods

2.1. Materials

The sources and composition of the used solvents in the ASA reaction mixture are shown in Table 1. These were similarly prepared as it was published by the authors previously [62,63]. In the ASA solution used for the crystallization experiments, 5% salicylic acid (SA) represented the impurity content of the flow synthesis solution. Since among the <5% amount of total byproducts – SA (<3%), acetylsalicylic anhydride (<1%), and others (<1%) – the amount of SA was the highest. The reaction mixture contained ASA in 91.9 mg/mL (0.097 g ASA/g solvent mixture) concentration and SA in 4.84 mg/mL concentration.

ASA (>99.0%) and SA (>99.0%) were obtained from Sigma Aldrich. The n-heptane (>96.0%) was purchased from Molar Chemicals. The acetonitrile (ACN, >99.9%) and methanol (MeOH, 99.9%) used for the HPLC measurements were obtained from Merck.

2.2. Experimental methods

2.2.1. The continuous plug flow crystallization

For mixing the ASA solution with antisolvent multiple mixer configurations – such as T- and Y-type mixer and coaxial mixer – were tested. The schematic drawing of the designed coaxial mixer is shown in Fig. 1.

The coaxial mixer was made from a T-type polytetrafluoroethylene (PTFE) connector with three internal thread connections with a 1/16″ (1.6 mm) thru-hole. One of the horizontal thru-holes was enlarged to 1.8 mm. A 1/32″ inner diameter (ID) × 1/16″ outer diameter (OD) (0.79 × 1.6 mm) PTFE tubing was led through the hole horizontally that was used for feeding the ASA solution continuously to the PFC. On the left side, the tubing was fitted perfectly in the thru-hole, while on the other side, the thru-hole was a bit larger. The perpendicular connection was used for feeding the antisolvent. Entering the modified T-type connector, the antisolvent can flow merely into the crystallizer through the enlarged thru-hole.

The continuous crystallization was performed in a PTFE tubing (2 mm ID, 3 mm OD) ordered from Upchurch Scientific. The TFR was fixed at a constant level of 10 mL/min or 25 mL/min. Therefore, to set the desired mean RT, the length of the applied pipe was modified. The following equation was used to calculate the length of tubing (l, cm) including the mean RT (t_{RT}, min), the area of the tube inner cross-section (A_{ID}, cm^2), and the TFR ($\dot{v}$, cm^{3}min^{-1}):

$$l = \frac{\sum \dot{v} * t_{RT}}{A_{ID}} \tag{1}$$

As the mean RT was set at 30, 60, and 90 s, the length of the tubing was ranged from 160 cm to 1200 cm. The whole tubing or only a part of the tubing was placed in a Bandelin Sonorex RK 510 type ultrasonic bath (ultrasonic peak power: 640 W, ultrasonic nominal power:

Table 1
Purity, V//V ratio, and source of the solvents in the reaction mixture.

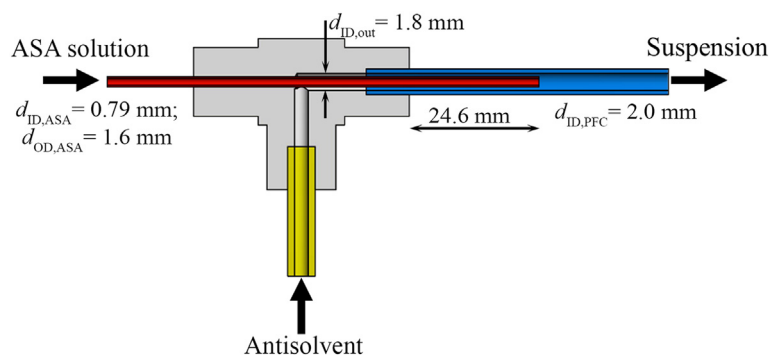|	Purity	V/V %	Source
Ethyl acetate (EtOAc)		79.5	
Acetic acid (AcOH)	99–100%	16.3	Merck Millipore
Ethanol (EtOH)	≥99%	3.8	
Phosphoric acid (H$_3$PO$_4$)	85 wt%	0.4	

Fig. 1. Schematic image of the coaxial mixer.

160 W) to provide intense and continuous mixing; and thus, to avoid clogging in the pipe. The frequency was maintained consistently at 35 kHz. The ultrasonic bath was filled with deionized water and ice if the experiment temperature was set at 1 °C. ASA solution was fed using a Jasco PU-980 HPLC pump. Heptane antisolvent was added in multiple amounts (2×, 4×, or 6×) for appropriate yield. Antisolvent was fed with a Syrris Asia syringe pump. The schematic image of PFC is shown in Fig. 2.

The suspension leaving the pipe was filtered directly using G4 glass filters connected to a continuously operating diaphragm pump. The crystals were dried at room temperature without washing until constant weight. Afterward, the tared filters containing the samples were weighed to calculate the yield of sample number X ($y_{s,X}$, %) with the following equations:

$$m_f = t_f \times \dot{V}_s \times c_s \tag{2}$$

$$y_{s,X} = \frac{m_s}{m_f} \times 100 \tag{3}$$

where m_f is the nominal fed ASA amount [g]; t_f is the feeding time [min]; $\dot{V}_s$ is the volumetric flow rate of ASA solution [mL/min]; c_s is the concentration of ASA solution [g/mL]; and m_s is the weight of the dried samples in g. The average yield (y_{Av}, %) and its standard deviation (*St. dev.*, %) was calculated as follows:

$$y_{Av} = \frac{\sum y_{s,X}}{n} \tag{4}$$

$$St.dev. = \sqrt{\frac{\sum (y_{s,X} - y_{Av})^2}{(n-1)}} \tag{5}$$

where n [−] is the number of samples.

The continuous experiments lasted for 1 or 1.5 h, which means at least 40 RTs depending on the size of the PFC. Each experiment was sampled 4 to 5 times at 2 to 5 min intervals.

2.2.2. Continuous crystallization experiments in PFC

To test the developed continuous PFC, three series of experiments were performed. In the 1st series of experiments, in order to investigate the effect of crystallization parameters (temperature, antisolvent to ASA solution ratio, mean RT) on product quality and quantity a 2 by 3 factorial design of the experiments (DoE) was applied. The entire tubing length was sonicated. Two parallel center point experiments were performed to investigate the reproducibility and repeatability of the results in the experimental region. The temperature was considered as a categorical variable as its level cannot be set continuously, thus at the center point, the experiments were performed both at 1 °C and 25 °C. The set levels of these parameters are detailed in Table 2. The experiments were performed in 4 days (3 exp./day) in randomized order. Other disturbing parameters were investigated through a blocking factor (day of performance). The TIBCO Statistica (version 13.5) program was used to evaluate the experimental results. The statistical analysis was performed at a 0.05 significance level.

In the 2nd series of experiments, the effect of US-assisted pipe length was investigated by placing only a part of the tubing into the ultrasonic bath reducing the pipe length treated with ultrasonic irradiation. The operation conditions were set to a central point of the 1st series of experiments (PF_13 – PF_21). The sonicated pipe length was varied between 320 and 15 cm (ultrasonication time: 60–2.8 s). Some experiments were carried out in 480 cm (PF_22 and PF_23) and 1200 cm (PF_24 and PF_25) PFCs (ID: 2.0 mm) sonicating the initial 20 cm of the tubing.

For the 3rd series of experiments, the TFR was increased to 25 mL/min to increase the productivity of the technology. Experiment PF_24
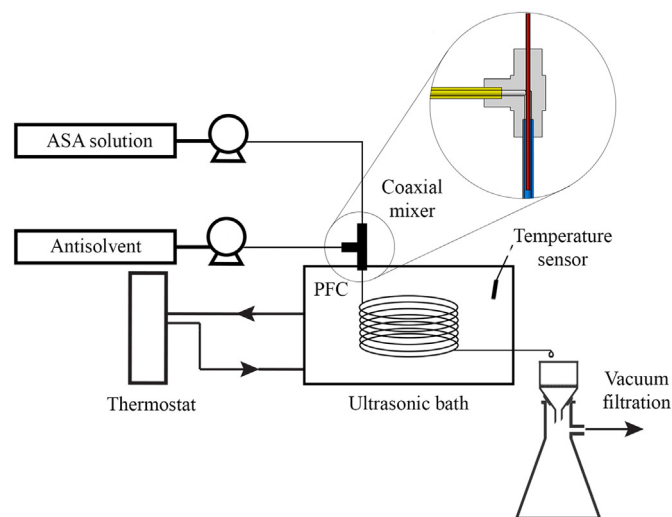

Fig. 2. Schematic image of PFC, when the entire tubing was sonicated.

Table 2
Levels of the investigated crystallization parameters in the 1st series of experiments (PF_1-PF_12).

	− (lower)	0 (central)	+ (upper)
Temperature [°C]	1	–	25
Antisolvent to ASA solution ratio [−]	2:1	4:1	6:1
Mean RT [sec] (tubing length [cm])	30 (160)	60 (320)	90 (480)

Table 3
Experimental conditions during the 2nd and 3rd series of experiments.

Series of exp.	ID of exp.	Tubing length [cm]	Sonicated tubing length [cm] (sonication time [sec])	TFR [mL/min]	T [°C]	AS/ASA ratio [−]	Mean RT [sec]
2nd	PF_13-PF_21	320	15–320 (2.8–60)	10	25	4:1	60
	PF_22	480	20 (3.8)	10	1	4:1	90
	PF_23	480	20 (3.8)	10	25	4:1	90
	PF_24[a]	1200	20 (1.5)	25	1	4:1	90
	PF_25[a]	1200	20 (1.5)	25	25	4:1	90
3rd	PF_26	1200	1200 (90)	25	1	4:1	90
	PF_27	1200	1200 (90)	25	25	4:1	90
	PF_28	480	480 (36)	25	25	4:1	36

[a] Experiment PF_24 and PF_25 are also included in the 2nd and 3rd series of experiments.

and PF_25 also belong to the 2nd and 3rd series of experiments. The operation conditions of the 2nd and 3rd series of experiments are summarized in Table 3.

2.2.3. Analysis of product quality

The purity of the product was investigated following the same HPLC method which was used in previous studies of the authors [62–64]. After filtration, the wet samples were dissolved in EtOH to make solutions 1 mg/mL concentration, which was further diluted (1:20 ratio) with a mixture of acetonitrile, methanol, and phosphoric acid (ACN: MeOH:H$_3$PO$_4$ in 92:8:0.5 v/v%). The HPLC measurements were performed on a Supelco Inertsil ODS-2 C18 column by the injection of 5 μL of the diluted sample and the eluent mixture (60% ACN and 40% water-H$_3$PO$_4$). The purity of the product was calculated based on the ASA and SA peak areas that were detected at 2.5 and 3.1 min retention time, respectively.

An offline Malvern Mastersizer 2000 equipped with a Malvern Scirocco 2000 dry powder feeder was used to measure CSD plot according to the method detailed in a previous publication of the authors [63]. During the 6 s measurement, approximately 100 mg dried samples were dispersed with 1 bar overpressure. Each sample was measured multiple times, enabling us to calculate the average and standard deviation of the D$_v$10, D$_v$50, and D$_v$90 values. In addition, a CKX53 inverse microscope was used to perform the visual observation of the crystals (magnification 4× or 10×).

3. Results and discussion

According to the preliminary experiments, approximately 25% yield could be obtained in the ultrasonicated PFC cooled to 1 °C in the absence of antisolvent. Thus, it was necessary to use an antisolvent to increase production in addition to cooling. One of the most critical steps during continuous antisolvent plug flow crystallization was the mixing of the antisolvent and ASA solution using a 2:1, 4:1, or 6:1 ratio. Multiple amounts of antisolvent are recommended for realizing high yield from the ASA solution. However, the relatively high supersaturation (0.9–4.0 calculated with $\frac{c_s}{c_s^*} - 1$, where c_s is the ASA solution concentration [g/mL], c_s^* is equilibrium solubility [g/mL]) in the mixing region caused the rapid blockage of the mixers. This phenomenon was experienced in all cases when typical mixing elements were used, such as T- and Y-type mixers. As a result, these conventional mixing elements were found to be inappropriate for use in a highly supersaturated system, such as the antisolvent crystallization of the fixed concentration ASA solution. The source of the difficulties during mixing with T- and Y-type mixers (that aid mixing by the frontal collision of fluids) is that, due to the different flow rates, back mixing could occur in the ASA solution feeding side. Therefore, the RT of the ASA solution increases in such cases leading to nucleation and clogging the mixing element. To solve this issue, we used a coaxial mixer that was effective in preventing the formation of such a stagnant zone and the blocking of the mixing element.

By investigating the PFC product in preliminary experiments, it was found that the product was crystalline, signs that refer to amorphous material content were not detected. The characterization of the PFC product (XRPD, DSC, and TGA) is detailed in Supplementary Materials. As the process was robust, we analyzed only one PF product.

In the next section, initially, the detailed characterization of product quality and quantity of the 1st series of experiments is presented regarding purity, yield, productivity, product size, and size distribution. Afterward, the effect of ultrasonicated tubing length and increased TFR is described focusing on the main differences compared to the 1st series of experiments.

3.1. Results in the 1st series of experiments

3.1.1. Characterization of product purity, process yield, and productivity

The developed crystallization technology was characterized regarding purification efficacy by analyzing the SA content of each sample of the 1st series of experiments with HPLC measurement. On average, the initial 5% SA impurity content was reduced to 0.67 ± 0.23% (Table 4). Neither of the investigated process parameters had a significant effect on the impurity content of the product in this experimental region. The cleaning efficacy of the ultrasonicated PFC system was proved to be appropriate, moreover, it could be further improved with washing.

The crystallization technology was characterized regarding yield and productivity as well (Table 4). The yield was constant during an experiment as each sample yield was similar with a relatively low standard deviation (<2.6%). Consequently, each sampling yield and productivity value were used to calculate the average yield and productivity and its standard deviation (eq 4. and 5.).

To reveal the process parameter effect on the product quantity, we performed statistical analysis. The levels of temperature, antisolvent to ASA solution ratio, and mean RT were modified according to the rules of DoE. At the same time, other disturbing factors that were not considered in the design were analyzed through the day of performance (blocking factor). Repeated center point measurements (PF_9, PF_10 and PF_11, PF_12) were performed to prove the repeatability and reproducibility of the crystallization experiments and to examine the curvature of the fitted model. The blocking factor proved to be not significant ($p >> 0.05$), therefore it was not considered in the further analysis. Table 5 summarizes p-values, the coefficient estimates, and the confidence intervals of the investigated factors and interactions. The coefficient describes the relationship (size and direction) between the given factor or factor interactions and the yield. The uncertainty of the estimated values is presented by the confidence intervals of the coefficients.

The temperature and antisolvent to ASA solution ratio have the most remarkable effect on yield, as it is proved by the Half normal probability plot (Fig. 3). However, the curvature and the interaction of temperature and antisolvent to ASA solution ratio seems statistically significant (p-value <0.05), these effects could be neglected compared to the scale of temperature and antisolvent to ASA solution ratio linear effects.

Table 4
Crystallization parameters, yield, productivity, SA content, and initial supersaturation (SS) of 1st series of experiment.

ID of exp.	Day of perf.	T [°C]	Antisolvent to ASA solution ratio [−]	Mean RT [sec]	Yield [%]	Productivity [g/h]	SA content [%]	Initial SS [−]
PF_1	1	1	2:1	30	70.9 ± 0.8	13.0 ± 0.1	0.7 ± 0.1	2.7
PF_2	3	1	2:1	90	70.0 ± 0.7	12.9 ± 0.1	0.7 ± 0.3	2.7
PF_3	4	1	6:1	30	88.9 ± 1.8	7.0 ± 0.1	0.7 ± 0.1	4.0
PF_4	2	1	6:1	90	86.3 ± 1.3	6.8 ± 0.1	0.8 ± 0.4	4.0
PF_5	2	25	2:1	30	48.6 ± 2.3	8.9 ± 0.4	0.6 ± 0.2	0.9
PF_6	3	25	2:1	90	50.4 ± 1.2	9.3 ± 0.2	0.5 ± 0.0	0.9
PF_7	1	25	6:1	30	76.3 ± 1.5	6.0 ± 0.1	0.7 ± 0.2	1.8
PF_8	4	25	6:1	90	77.6 ± 2.0	6.1 ± 0.2	0.8 ± 0.3	1.8
PF_9	2	1	4:1	60	82.9 ± 2.6	9.0 ± 0.5	0.7 ± 0.2	2.8
PF_10	4	1	4:1	60	80.2 ± 0.7	8.8 ± 0.1	0.4 ± 0.2	2.8
PF_11	1	25	4:1	60	68.5 ± 1.3	7.4 ± 0.3	0.7 ± 0.2	1.4
PF_12	3	25	4:1	60	66.7 ± 0.8	7.4 ± 0.1	0.8 ± 0.3	1.4

As the ultrasonication initiates homogeneous and rapid primary nucleation after the mixing zone, the mean RT has no effect on yield in the investigated experimental region. It was observed that the suspension started to form 15–20 cm after the coaxial mixer in every experiment, independently from the operating conditions. Considering all the above, the yield (y, %) can be calculated with the following reduced linear model:

$$y = 57.61 - 0.56z_T + 5.50z_{AS/ASA} \qquad (6)$$

where z_T represents the temperature [°C], and $z_{AS/ASA}$ means antisolvent to ASA solution ratio [−]. According to the diagnostic figures, the assumptions of the model were fulfilled; thus, the equation is considered reliable. As the curvature was found statistically significant, in order to describe the relationship between the factors and the dependent variable mathematically more precisely, it might be recommended to examine the effect of quadratic terms as well. To represent the effect of temperature and antisolvent to ASA solution ratio on yield, we generated a Response Surface using the TIBCO Statistica program (Fig. 4).

In the 1st series of experiments, the TFR was set 10 mL/min constantly, and the antisolvent to ASA solution ratio was modified between 2 and 6, therefore the alteration of productivity was reversed to the antisolvent to ASA solution ratio and also the temperature. The productivity in the 1st series of experiments was ranged from 6.0 to 13.0 g/h.

3.1.2. Characterization of crystal size, habit, and CSD

We experienced that the ultrasonication initiates the primary nucleation and then prevents the aggregation of the crystals. The growth of the crystals was not dominant in the ultrasonicated PFC. Homogeneous, columnar, small crystal size products with narrow and unimodal CSD were produced. Each sample of an experiment (collected after 3, 15, 35, 60, and 90 min) contained particles with similar crystal habit, size, and CSD; thus, the product morphology was not altered during the experiments.

Neither yield nor crystal habit, size, and CSD were not changing during the operation of the PFC. The product quality and quantity were stable during the entire operation according to the utilized sampling method; thus, it can be assumed that the steady-state operation

condition was attained immediately after the process started. To precisely investigate the operation startup, in-situ process monitoring technology with sec magnitude turnaround time should be applied to reveal the sec magnitude changes in product quality and quantity. Since no startup period was observed in any case, no oscillation of crystal size occurred either. Considering this, for the investigation of product crystal size and CSD, each sampling point D_v10, D_v50, and D_v90 values were used to calculate the average and standard deviation values. The results are summarized in Fig. 5.

According to Fig. 5, the antisolvent to ASA solution ratio slightly affects crystal size and CSD, while temperature and mean RT did not alter the product morphology. By applying a higher amount of antisolvent the produced suspension was diluter just as it could be tracked in the productivity results. The higher productivity was measured when lower antisolvent to ASA solution ratio was set. It could be assumed that the abrasion effect of the collapse of the ultrasonication-induced cavitation bubbles is more pronounced in a denser crystallization medium resulting in relatively smaller crystal sizes. However, as shown in Table 6 illustrating the effect of antisolvent to ASA solution ratio, the difference between D_v90 values is maximum 12 μm. This difference in size could not change the technological properties (such as compressibility and dissolution properties) of the products; therefore, it is considered insignificant in the aspect of the product usability. The product habit and the shape of CSD curves were very similar in each product regardless of the applied antisolvent amount.

The reason for the insignificance of investigated parameters regarding crystal size, habit, and CSD was the dominance of low-frequency ultrasonication that accelerates nucleation. As the circumstances of ultrasonication were constant during the experiments, it could cause the absence of crystal size modification effect of the process parameters. Consequently, the robustness of this technology is much higher, while it enables the production of smaller crystals with narrow CSD compared to previously investigated overflow MSMPR systems [62]. However, the compressibility of these products is presumably worse, while the dissolution rate can be much higher due to the increased specific crystal surface area. This assumption is also supported by the dissolution model built and published by Nagy and co-workers to the same ASA reaction mixture [65].

3.2. Evaluation of the effect of sonicated tubing length

By sonicating a shorter tubing section, the ultrasonication capacity requirement of the technology is being reduced, which can be important, especially during scale-up. In the 1st series of experiments, it was observed that the crystallization solution started to be cloudy 15–20 cm after the mixing zone. Therefore, we were interested in the minimum sonicated tubing length that was necessary for stable crystallization. In the 2nd series of experiments, the sonicated tubing length was
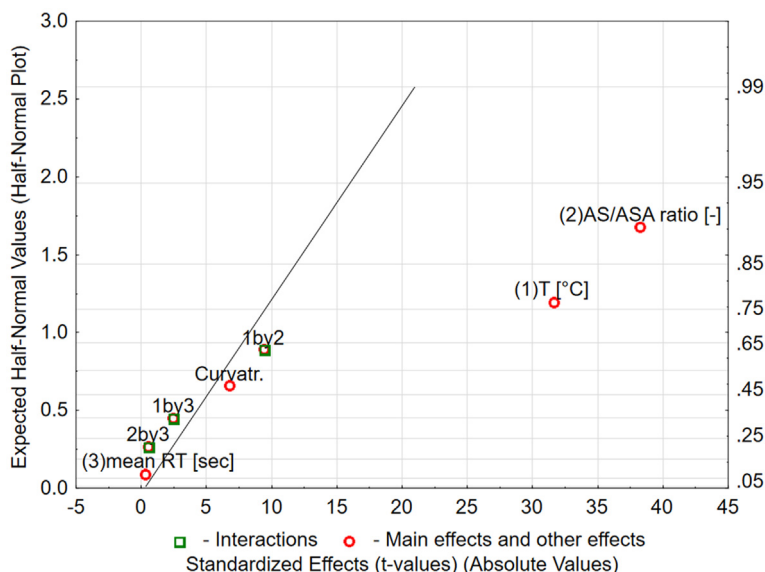
Table 5
The p-values, estimates, and confidence intervals of the model coefficients ($R^2 = 0.986$).

Factors	Coeff.	p-value	−95% conf. limit	+95% conf. limit
Mean	71.00	0.000	70.42	71.59
Curvature	3.42	0.000	2.39	4.45
T [°C] (1)	−7.51	0.000	−8.00	−7.03
AS/ASA solution [−] (2)	11.01	0.000	10.42	11.59
Mean RT [sec] (3)	0.08	0.794	−0.51	0.66
1 by 2	2.69	0.000	2.11	3.28
1 by 3	0.70	0.019	0.12	1.29
2 by 3	−0.15	0.608	−0.73	0.43

Fig. 3. Half normal probability plot aids to select significant effects.

decreased stepwise from 320 to 15 cm while the sonication effect on yield, crystal size, and CSD was investigated. The summary of the results is detailed in Fig. 6.

It is shown in Fig. 6(a), that by reducing the sonicated section of the pipe, the yield was not altered significantly between 320 and 20 cm ultrasonicated tubing length. When the sonicated part of the tubing was reduced under 20 cm the nucleation could not initiate. In this case, crystal nucleation was started spontaneously after some minutes of operation and resulted in clogging of the tube at random locations. In these circumstances, crystals were not produced, and the continuous operation was not accomplished. This phenomenon was also experienced in the case of the absence of ultrasonication. Consequently, it could be stated that for the stable and robust operation of the applied continuous crystallization system at least the first 20 cm tubing section must be sonicated. Sonication-induced homogeneous mixing is essential for avoiding

spontaneous nucleation, which could lead to clogging of the system without mixing. The US ideally applied in the initial tube section ensures agitation, thus, initiating homogeneous nucleation.

US assists the microbubble coalescence inside the PFC causing continuous bubble formation shortly after the mixing zone. The closely spaced bubbles fused and filled the entire cross-sectional of the pipe. As a result, 5–10 cm long slug sections were created in the crystallizer separated by bubbles, which could narrow the residence time distribution of the liquid and solid phases as well compared to standard tubular reactors. Due to this coalescence phenomenon that occurred during crystallization, the process was similar to slug flow crystallization in CSFCs [66], except that the volume of the slugs were not controlled.

The effect of the ultrasonicated tubing length on the yield was also analyzed statistically with one-way ANOVA. The sonicated tube section length was considered as a fixed effect. The null hypothesis stated that
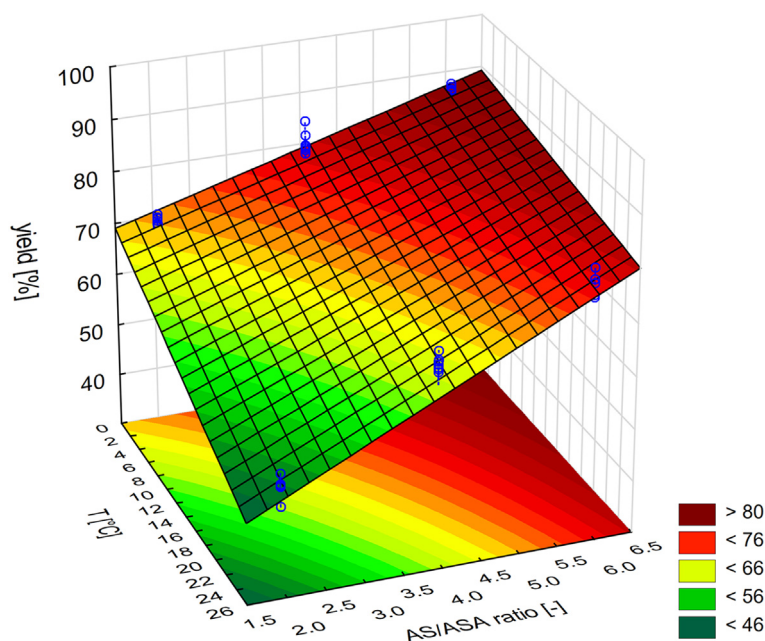

Fig. 4. Response Surface presenting yield as a function of temperature and antisolvent to ASA solution ratio in the investigated experimental region.
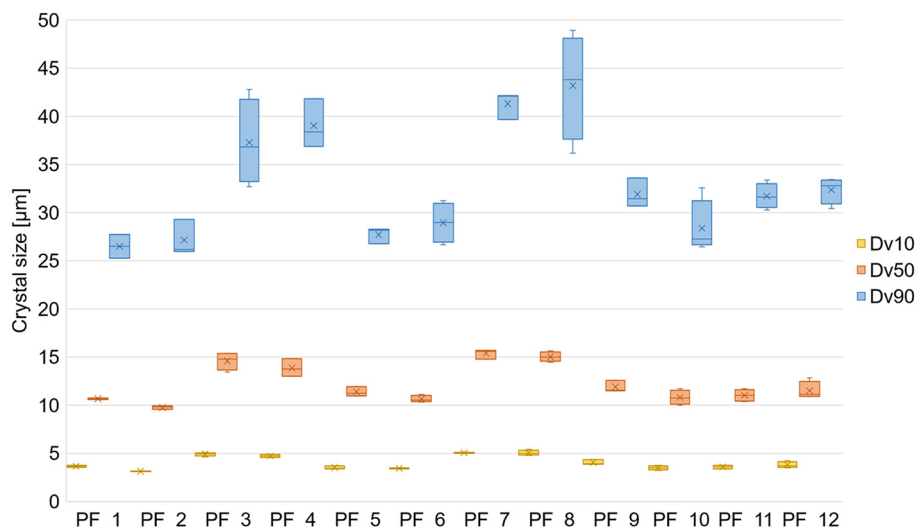
Fig. 5. Mean and standard deviation of D_v10, D_v50, and D_v90 values in the 1st experimental series.

the tubing length did not affect product quantity. According to the statistical analysis, the null hypothesis failed ($p = 0.000025$). In this case, however, the standard deviation of yield in the entire 2nd experimental series was in the same magnitude as the standard deviation of an experiment in the 1st series of experiments, therefore the effect of yield was considered professionally insignificant.

The D_v90 values were dropped from 33.3 ± 3.2 μm (sonicated tube length: 320 cm) to 25.4 ± 3.3 μm (sonicated tube length: 20 cm). Therefore, the crystal size and CSD alteration were also not remarkable by reducing the sonicated pipe length. However, by reducing the ultrasonicated tube length, the consistency of the product showed some differences. The particles which were treated by shorter sonication stuck more likely together, forming agglomerates that could be observed in microscopic pictures but that disintegrated easily during the CSD measurement. The microscopic pictures and CSD plots of these products are presented in Table 7.
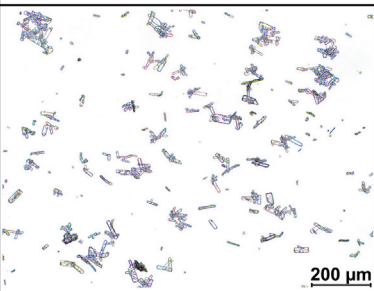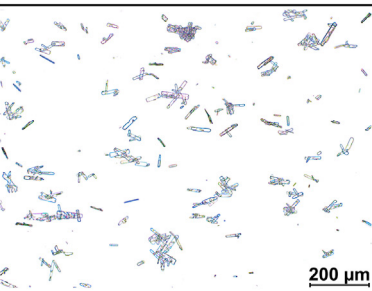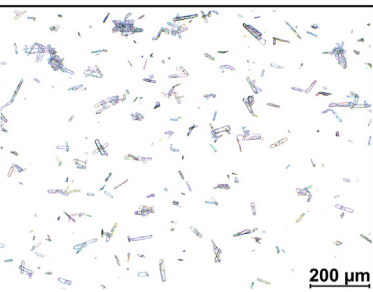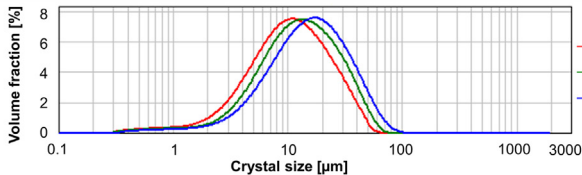
Continuous crystallizations were also performed in 480 cm and 1200 cm long PFCs with increased TFR while only the initial 20 cm of the equipment was sonicated. With this operation, it was managed to produce products with constant quality and quantity. A more detailed characterization of these experiments is found in Section 3.3.

3.3. Examining the scalability

The possibility of the system scaling up at an increased flow rate was investigated in the 3rd series of experiments. The TFR was increased from 10 mL/min to 25 mL/min using a 1200 cm and a 480 cm tubing to set the mean RT to 90 and 36 s. The product parameters are summarized in Table 8.

Increasing the TFR to 25 mL/min, the yield value was similar to the 10 mL/min central point experiments at both temperatures. In PF_28, when increased TFR was coupled with reduced RT, the yield was similar

Table 6
Microscopic pictures, CSD plots, and D_v-values of PF_6, PF_12, and PF_7 experiments.

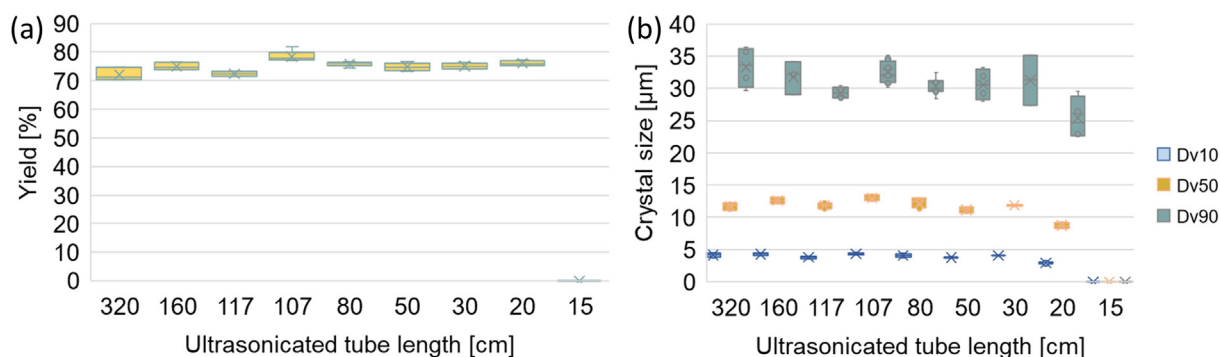| PF_6 T:25°C; AS/ASA: 2:1; RT: 90 sec			PF_12 T:25°C; AS/ASA: 4:1; RT: 60 sec			PF_7 T:25°C; AS/ASA: 6:1; RT:30 sec		
D_v10 [μm]	D_v50 [μm]	D_v90 [μm]	D_v10 [μm]	D_v50 [μm]	D_v90 [μm]	D_v10 [μm]	D_v50 [μm]	D_v90 [μm]
3.4 ± 0.1	10.6 ± 0.4	28.9 ± 2.1	3.8 ± 0.3	11.5 ± 0.9	32.3 ± 1.4	5.0 ± 0.0	15.2 ± 0.6	40.9 ± 1.7

Fig. 6. Box plot diagrams of (a) yield and (b) D_v-values as a function of ultrasonicated tube length altered from 320 cm (entire tubing) to 15 cm (Parameters: tubing length: 320 cm; T: 25 °C; AS/ASA: 4:1; RT: 60 s).

to the mentioned central point results. It could be assumed that the increased TFR did not alter the yield remarkably. However, slight differences could occur due to the fluctuations between repeated measurements. At the same time, productivity was highly increased compared to the 1st series of experiments due to higher feeding volume.

According to the microscopic pictures and the CSD plots presented in Table 8, the major peak in the CSD plots was in a similar size range compared to other PF products, but the crystals could agglomerate in a small amount when higher TFR was applied. An explanation for this is that higher TFR and ultrasonication together could result in more intense mixing, hereby shorter induction time and it could also lead to an increased agglomeration by increased frequency of crystal-crystal collision. Meanwhile, the applied sonication might not support the deagglomeration due to the short RT [67], which would be facilitated by higher ultrasonic power and longer RT [68]. The agglomeration was not disturbing the continuous operation, therefore the experiments with increased 25 mL/min TFR remained robust and downtime-free as well, even when the sonicated tubing length was reduced. This small amount of agglomerates could also not modify the technological properties of the product.

It was found that by sonicating the 20 cm tubing section – i.e., applying 1.5 s sonication time – the yield remained unchanged and the average crystal size varied negligibly within the standard deviation of D_v (Table 9). The ultrasonication of the initial 20 cm tubing was sufficient for inducing primary nucleation, in this way, the maintenance-free continuous operation could still be accomplished. This could reduce the specific sonication requirement of the technology, which is important during scale-up.
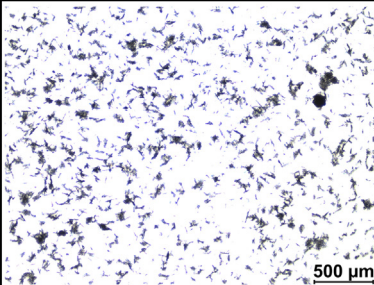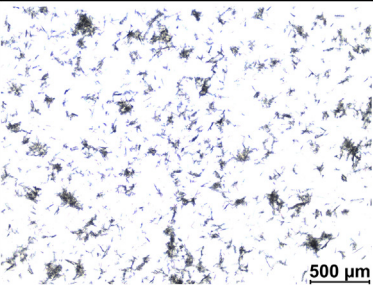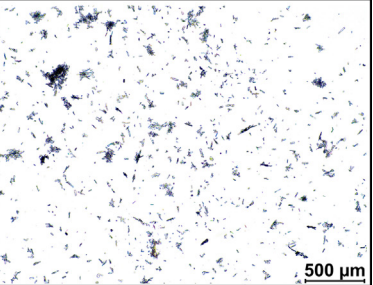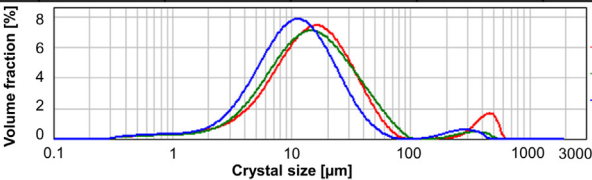
4. Conclusions

Continuous antisolvent and combined cooling and antisolvent crystallization was performed in an ultrasonicated PFC, which was developed to separate and purify ASA from a multicomponent flow synthesis product. An instantaneous clogging of the tubular crystallizer was observed with conventionally used mixer elements (X-, Y-type mixers), thereby the assembled PFC was equipped with a coaxial mixer, which successfully prevented clogging of the mixing region. In the 1st series of experiments, the process parameter (temperature, antisolvent to ASA solution ratio, mean RT) dependence on product quality (purity, crystal size, habit, CSD) and quantity (yield,

Table 7
Microscopic pictures and CSD plots of the product obtained in entirely (320 cm) or partially (107 cm or 20 cm ultrasonicated section) sonicated PFCs.

D_v10 [μm]	D_v50 [μm]	D_v90 [μm]	D_v10 [μm]	D_v50 [μm]	D_v90 [μm]	D_v10 [μm]	D_v50 [μm]	D_v90 [μm]
4.2 ± 0.3	11.7 ± 0.6	33.3 ± 3.2	4.3 ± 0.2	13 ± 0.4	32.4 ± 2	2.9 ± 0.1	8.7 ± 0.4	25.4 ± 3.3

Table 8
Product quality and quantity of experiments applying 25 mL/min TFR.

PF_26 T:1°C; AS/ASA: 4:1; RT: 90 sec			PF_27 T:25°C; AS/ASA: 4:1; RT:90 sec			PF_28 T:25°C; AS/ASA: 4:1; RT: 36 sec		
Yield								
80.7 ± 1.3%			62.0 ± 1.8%			66.5 ± 0.6%		
Productivity								
22.3 ± 0.4 g/h			17.1 ± 0.5 g/h			18.3 ± 0.2 g/h		
D_v10 [μm]	D_v50 [μm]	D_v90 [μm]	D_v10 [μm]	D_v50 [μm]	D_v90 [μm]	D_v10 [μm]	D_v50 [μm]	D_v90 [μm]
4.6 ± 0.1	15.2 ± 0.8	43.2 ± 2.6	4.2 ± 0.4	13.3 ± 1.2	37.7 ± 5.3	3.8 ± 0.2	11.2 ± 0.5	30.3 ± 2.4

productivity) were examined. It was found that the quality of the crystals could not be modified significantly with either of the process parameters since the ultrasonication-initiated rapid primary nucleation dominated during the process. With heptane antisolvent small, columnar crystals (< 50 μm) with narrow and unimodal CSD were produced with appropriate purity (99.33 ± 0.23%). Concerning the quantity of products, the technology operated with 49–89% yield and 6–13 g/h productivity. According to the statistical analysis, the yield was mainly influenced by the amount of antisolvent and the temperature. A linear model was described to predict the yield in other points of the investigated experimental region.

We studied the system by reducing the sonicated tubing length to find the minimum ultrasonic-irradiated tubing length for the stable operation, which could be important in the aspect of industrial application of the developed technology. It could be concluded that the sonication of the first 20 cm right after the coaxial mixer was enough to reach the same yield and product quality as in the 1st experimental series (the entire pipe was ultrasonicated). It is consistent with the observation that the steady-state onset was immediately after the operation start (start-up phase did not occur). By studying the possibility of scaling up through increasing the TFR (from 10 mL/min to 25 mL/min), the productivity was more than doubled (from 7.4–9.0 g/h to 17.1–22.3 g/h) without changing in product quality or losing the robustness of the technology. The productivity could be further increased with additional pump capacity.

The developed technology enables to perform the continuous crystallization of a multi-component system featured with high supersaturation and rapid kinetic processes without clogging of the tubular crystallizer. As a result, small particles with homogeneous and narrow CSD can be produced, therefore this technology could gain a prominent role in improving the dissolution rate of poorly water-soluble drug substances. A further strength of the developed ultrasonicated PFC is its robustness enabling it to produce crystals with constant quality and high quantity regardless of process parameters in the *sec* magnitude RT. The concept of promoting easy downstream processing of the crystals, produced this way, needed further development, which is among our plans.

CRediT authorship contribution statement

Kornélia Tacsi: Conceptualization, Methodology, Investigation, Validation, Visualization, Writing – original draft, Writing – review & editing. **György Stoffán:** Investigation. **Éva Pusztai:** Formal analysis, Writing – review & editing. **Brigitta Nagy:** Conceptualization. **András Domokos:** Conceptualization, Writing – review & editing. **Botond Szilágyi:** Conceptualization, Writing – review & editing. **Zsombor Kristóf Nagy:** Conceptualization. **György Marosi:** Conceptualization, Supervision, Writing – review & editing. **Hajnalka Pataki:** Conceptualization, Methodology, Supervision, Writing – review & editing.

Declaration of Competing Interest

The authors declare that they have no known competing financial interests or personal relationships that could have appeared to influence the work reported in this paper.

Table 9
Summary of experiment PF_24 and PF_25 results.

ID of exp.	Yield [%]	Productivity [g/h]	D_v10	D_v50	D_v90
PF_24	81.3 ± 1.2	22.4 ± 0.3	4.8 ± 0.2	13.1 ± 0.5	33.7 ± 4.9
PF_25	69.7 ± 1.3	19.2 ± 0.4	2.9 ± 0.1	9.2 ± 0.4	34.2 ± 7.3

the FIEK_16 funding scheme. Hajnalka Pataki is thankful for the János Bolyai Research Scholarship of the Hungarian Academy of Sciences. This work was financially supported by the National Research, Development, and Innovation Office of Hungary (OTKA PD-121143, KH-129584, FK-132133). The research was also supported by the ÚNKP-20-3-I-BME-310 and the ÚNKP-20-5-BME-307 New National Excellence Program of the Ministry for Innovation and Technology from the source of the National Research, Development, and Innovation Fund.

Appendix A. Supplementary data

Supplementary data to this article can be found online at https://doi.org/10.1016/j.powtec.2022.117255.

References

[1] G.D. Hadiwinoto, P.C.L. Kwok, H.H.Y. Tong, S.N. Wong, S.F. Chow, R. Lakerveld, Integrated continuous plug-flow crystallization and spray drying of pharmaceuticals for dry powder inhalation, Ind. Eng. Chem. Res. 58 (2019) 16843–16857, https://doi.org/10.1021/acs.iecr.9b01730.
[2] J. Chen, B. Sarma, J.M.B. Evans, A.S. Myerson, Pharmaceutical crystallization, Cryst. Growth Des. 11 (2011) 887–895, https://doi.org/10.1021/cg101556s.
[3] T. Wang, H. Lu, J. Wang, Y. Xiao, Y. Zhou, Y. Bao, H. Hao, Recent progress of continuous crystallization, J. Ind. Eng. Chem. 54 (2017) 14–29, https://doi.org/10.1016/j.jiec.2017.06.009.
[4] S. Ferguson, G. Morris, H. Hao, M. Barrett, B. Glennon, Characterization of the antisolvent batch, plug flow and MSMPR crystallization of benzoic acid, Chem. Eng. Sci. 104 (2013) 44–54, https://doi.org/10.1016/j.ces.2013.09.006.
[5] T.-T.C. Lai, J. Cornevin, S. Ferguson, N. Li, B.L. Trout, A.S. Myerson, Control of polymorphism in continuous crystallization via mixed suspension mixed product removal systems cascade design, Cryst. Growth Des. 15 (2015) 3374–3382, https://doi.org/10.1021/acs.cgd.5b00466.
[6] G. Power, G. Hou, V.K. Kamaraju, G. Morris, Y. Zhao, B. Glennon, Design and optimization of a multistage continuous cooling mixed suspension, mixed product removal crystallizer, Chem. Eng. Sci. 133 (2015) https://doi.org/10.1016/j.ces.2015.02.014.
[7] Y. Yang, Z.K. Nagy, Combined cooling and antisolvent crystallization in continuous mixed suspension, mixed product removal cascade crystallizers: steady-state and startup optimization, Ind. Eng. Chem. Res. 54 (2015) 5673–5682, https://doi.org/10.1021/ie5034254.
[8] H. Takiyama, M. Matsuoka, Design of seed crystal specifications for start-up operation of a continuous MSMPR crystallizer, Powder Technol. 121 (2001) 99–105, https://doi.org/10.1016/S0032-5910(01)00381-3.
[9] A. Majumder, Z.K. Nagy, Fines removal in a continuous plug flow crystallizer by optimal spatial temperature profiles with controlled dissolution, AICHE J. 59 (2013) 4582–4594.
[10] L. Zhao, V. Raval, N.E.B. Briggs, R.M. Bhardwaj, T. McGlone, I.D.H. Oswald, A.J. Florence, From discovery to scale-up: α-lipoic acid: nicotinamide co-crystals in a continuous oscillatory baffled crystalliser, CrystEngComm 16 (2014) 5769–5780, https://doi.org/10.1039/c4ce00154k.
[11] R. Vacassy, J. Lemaître, H. Hofmann, J.H. Gerlings, Calcium carbonate precipitation using new segmented flow tubular reactor, AICHE J. 46 (2000) 1241–1252, https://doi.org/10.1002/aic.690460616.
[12] M.O. Besenhard, P. Neugebauer, O. Scheibelhofer, J.G. Khinast, Crystal engineering in continuous plug-flow crystallizers, Cryst. Growth Des. 17 (2017) 6432–6444, https://doi.org/10.1021/acs.cgd.7b01096.
[13] M. Mou, H. Li, B.-S. Yang, M. Jiang, Continuous generation of millimeter-sized glycine in non-seeded millifluidic slug flow, Crystals. 9 (2019) 412.
[14] M. Mou, M. Jiang, Fast continuous non-seeded cooling crystallization of glycine in slug flow: pure α-form crystals with narrow size distribution, J. Pharm. Innov. 15 (2020) 281–294, https://doi.org/10.1007/s12247-020-09438-0.
[15] C.J. Brown, T. Mcglone, S. Yerdelen, V. Srirambhatla, F. Mabbott, R. Gurung, M.L. Briuglia, B. Ahmed, H. Polyzois, J. Mcginty, F. Perciballi, D. Fysikopoulos, P. Macfhionnghaile, H. Siddique, V. Raval, T.S. Harrington, A.D. Vassileiou, M. Robertson, E. Prasad, A. Johnston, B. Johnston, A. Nordon, J.S. Srai, G. Halbert, J.H. Ter Horst, C.J. Price, C.D. Rielly, J. Sefcik, A.J. Florence, Enabling precision manufacturing of active pharmaceutical ingredients: workflow for seeded cooling continuous crystallisations, Mol. Syst. Des. Eng. 3 (2018) 518–549, https://doi.org/10.1039/c7me00096k.
[16] B. Wood, K.P. Girard, C.S. Polster, D.M. Croker, Progress to date in the design and operation of continuous crystallization processes for pharmaceutical applications, Org. Process. Res. Dev. 23 (2019) 122–144, https://doi.org/10.1021/acs.oprd.8b00319.
[17] Y. Wang, M. Su, Y. Bai, Mechanism of glycine crystal adhesion and clogging in a continuous tubular crystallizer, Ind. Eng. Chem. Res. 59 (2020) 25–33, https://doi.org/10.1021/acs.iecr.9b05977.
[18] Y. Zhao, V.K. Kamaraju, G. Hou, G. Power, P. Donnellan, B. Glennon, Kinetic identification and experimental validation of continuous plug flow crystallisation, Chem. Eng. Sci. 133 (2015) 106–115, https://doi.org/10.1016/j.ces.2015.02.019.
[19] M. Ståhl, B.L. Åslund, Å.C. Rasmuson, Reaction crystallization kinetics of benzoic acid, AICHE J. 47 (2001) 1544–1560, https://doi.org/10.1002/aic.690470708.
[20] H. Li, H. Li, Z. Guo, Y. Liu, The application of power ultrasound to reaction crystallization, Ultrason. Sonochem. 13 (2006) 359–363, https://doi.org/10.1016/j.ultsonch.2006.01.002.
[21] R.J.P. Eder, E.K. Schmitt, J. Grill, S. Radl, H. Gruber-Woelfler, J.G. Khinast, Seed loading effects on the mean crystal size of acetylsalicylic acid in a continuous-flow crystallization device, Cryst. Res. Technol. 46 (2011) 227–237, https://doi.org/10.1002/crat.201000634.
[22] R.J.P. Eder, S. Radl, E. Schmitt, S. Innerhofer, M. Maier, H. Gruber-Woelfler, J.G. Khinast, Continuously seeded, continuously operated tubular crystallizer for the production of active pharmaceutical ingredients, Cryst. Growth Des. 10 (2010) 2247–2257, https://doi.org/10.1021/cg9015788.
[23] K.J. Kim, J.K. Kim, Nucleation and supersaturation in drowning-out crystallization using a T-mixer, Chem. Eng. Technol. 29 (2006) 951–956, https://doi.org/10.1002/ceat.200600081.
[24] S. Ferguson, G. Morris, H. Hao, M. Barrett, B. Glennon, In-situ monitoring and characterization of plug flow crystallizers, Chem. Eng. Sci. 77 (2012) 105–111, https://doi.org/10.1016/j.ces.2012.02.013.
[25] C. Lindenberg, J. Schöll, L. Vicum, M. Mazzotti, J. Brozio, Experimental characterization and multi-scale modeling of mixing in static mixers, Chem. Eng. Sci. 63 (2008) 4135–4149, https://doi.org/10.1016/j.ces.2008.05.026.
[26] C.A. Da Rosa, R.D. Braatz, Multiscale modeling and simulation of macromixing, micromixing, and crystal size distribution in radial mixers/crystallizers, Ind. Eng. Chem. Res. 57 (2018) 5433–5441, https://doi.org/10.1021/acs.iecr.8b00359.
[27] V. Svoboda, P. Macfhionnghaile, J. McGinty, L.E. Connor, I.D.H. Oswald, J. Sefcik, Continuous cocrystallization of benzoic acid and isonicotinamide by mixing-induced supersaturation: exploring opportunities between reactive and antisolvent crystallization concepts, Cryst. Growth Des. 17 (2017) 1902–1909, https://doi.org/10.1021/acs.cgd.6b01866.
[28] P. MacFhionnghaile, V. Svoboda, J. McGinty, A. Nordon, J. Sefcik, Crystallization diagram for antisolvent crystallization of lactose: using design of experiments to investigate continuous mixing-induced supersaturation, Cryst. Growth Des. 17 (2017) 2611–2621, https://doi.org/10.1021/acs.cgd.7b00136.
[29] C. Pirkle, L.C. Foguth, S.J. Brenek, K. Girard, R.D. Braatz, Computational fluid dynamics modeling of mixing effects for crystallization in coaxial nozzles, Chem. Eng. Process. Process Intensif. 97 (2015) 213–232, https://doi.org/10.1016/j.cep.2015.07.006.
[30] M. Jiang, Z. Zhu, E. Jimenez, C.D. Papageorgiou, J. Waetzig, A. Hardy, M. Langston, R.D. Braatz, Continuous-flow tubular crystallization in slugs spontaneously induced by hydrodynamics, Cryst. Growth Des. 14 (2014) 851–860, https://doi.org/10.1021/cg401715e.
[31] B. Giroire, S. Marre, A. Garcia, T. Cardinal, C. Aymonier, Continuous supercritical route for quantum-confined GaN nanoparticles, React. Chem. Eng. 1 (2016) 151–155, https://doi.org/10.1039/c5re00039d.
[32] R. Baber, L. Mazzei, N.T.K. Thanh, A. Gavriilidis, An engineering approach to synthesis of gold and silver nanoparticles by controlling hydrodynamics and mixing based on a coaxial flow reactor, Nanoscale. 9 (2017) 14149–14161, https://doi.org/10.1039/c7nr04962e.
[33] J. Sui, J. Yan, D. Liu, K. Wang, G. Luo, Continuous synthesis of nanocrystals via flow chemistry technology, Small. 16 (2020) 1–23, https://doi.org/10.1002/smll.201902828.
[34] M. Kreimer, M. Zettl, I. Aigner, T. Mannschott, P. Van Der Wel, J.G. Khinast, M. Krumme, Performance characterization of static mixers in precipitating environments, Org. Process. Res. Dev. 23 (2019) 1308–1320, https://doi.org/10.1021/acs.oprd.8b00267.
[35] J. Lu, J.D. Litster, Z.K. Nagy, Nucleation studies of active pharmaceutical ingredients in an air-segmented microfluidic drop-based crystallizer, Cryst. Growth Des. 15 (2015) 3645–3651, https://doi.org/10.1021/acs.cgd.5b00150.
[36] A.B. Corradi, F. Bondioli, A.M. Ferrari, B. Focher, C. Leonelli, Synthesis of silica nanoparticles in a continuous-flow microwave reactor, Powder Technol. 167 (2006) 45–48, https://doi.org/10.1016/j.powtec.2006.05.009.
[37] M.N. Hussain, S. Baeten, J. Jordens, L. Braeken, T. Van Gerven, Process intensified anti-solvent crystallization of o-aminobenzoic acid via sonication and flow, Chem. Eng. Process. Process Intensif. 149 (2020) 107823 https://doi.org/10.1016/j.cep.2020.107823.
[38] Y. Mao, F. Li, T. Wang, X. Cheng, G. Li, D. Li, X. Zhang, H. Hao, Enhancement of lysozyme crystallization under ultrasound field, Ultrason. Sonochem. 63 (2020), 104975https://doi.org/10.1016/j.ultsonch.2020.104975.
[39] C. Fang, W. Tang, S. Wu, J. Wang, Z. Gao, J. Gong, Ultrasound-assisted intensified crystallization of L-glutamic acid: crystal nucleation and polymorph transformation, Ultrason. Sonochem. 68 (2020) 105227 https://doi.org/10.1016/j.ultsonch.2020.105227.
[40] J. Jordens, B. Gielen, C. Xiouras, M.N. Hussain, G.D. Stefanidis, L.C.J. Thomassen, L. Braeken, T. Van Gerven, Sonocrystallisation: observations, theories and guidelines, Chem. Eng. Process. Process Intensif. 139 (2019) 130–154, https://doi.org/10.1016/j.cep.2019.03.017.
[41] M.D.L. de Castro, F. Priego-Capote, Ultrasound-assisted crystallization (sonocrystallization), Ultrason. Sonochem. 14 (2007) 717–724, https://doi.org/10.1016/j.ultsonch.2006.12.004.
[42] J. Jordens, E. Canini, B. Gielen, T. Van Gerven, L. Braeken, Ultrasound assisted particle size control by continuous seed generation and batch growth, Crystals. 7 (2017) 1–20, https://doi.org/10.3390/cryst7070195.
[43] L.M. Belca, A. Ručigaj, D. Teslič, M. Krajnc, The use of ultrasound in the crystallization process of an active pharmaceutical ingredient, Ultrason. Sonochem. 58 (2019) 104642https://doi.org/10.1016/j.ultsonch.2019.104642.
[44] M. Kakran, N.G. Sahoo, L. Li, Z. Judeh, Particle size reduction of poorly water soluble artemisinin via antisolvent precipitation with a syringe pump, Powder Technol. 237 (2013) 468–476, https://doi.org/10.1016/j.powtec.2012.12.029.

[45] H.U. Rodríguez Vera, F. Baillon, F. Espitalier, P. Accart, O. Louisnard, Crystallization of α-glycine by anti-solvent assisted by ultrasound, Ultrason. Sonochem. 58 (2019) 104671 https://doi.org/10.1016/j.ultsonch.2019.104671.

[46] R. Ambrus, N.N. Amirzadi, Z. Aigner, P. Szabó-Révész, Formulation of poorly water-soluble gemfibrozil applying power ultrasound, Ultrason. Sonochem. 19 (2012) 286–291, https://doi.org/10.1016/j.ultsonch.2011.07.002.

[47] N. Belkacem, M.A. Sheikh Salem, H.S. AlKhatib, Effect of ultrasound on the physico-chemical properties of poorly soluble drugs: Antisolvent sonocrystallization of ketoprofen, Powder Technol. 285 (2015) 16–24, https://doi.org/10.1016/j.powtec.2015.06.058.

[48] O. Narducci, A.G. Jones, E. Kougoulos, Continuous crystallization of adipic acid with ultrasound, Chem. Eng. Sci. 66 (2011) 1069–1076, https://doi.org/10.1016/j.ces.2010.12.008.

[49] P. Sayan, S.T. Sargut, B. Kiran, Effect of ultrasonic irradiation on crystallization kinetics of potassium dihydrogen phosphate, Ultrason. Sonochem. 18 (2011) 795–800, https://doi.org/10.1016/j.ultsonch.2010.11.003.

[50] H. Siddique, C.J. Brown, I. Houson, A.J. Florence, Establishment of a continuous sonocrystallization process for lactose in an oscillatory baffled crystallizer, Org. Process. Res. Dev. 19 (2015) 1871–1881, https://doi.org/10.1021/acs.oprd.5b00127.

[51] B. Rimez, R. Debuysschère, B. Scheid, On the effect of flow restrictions on the nucleation behavior of molecules in tubular flow Nucleators, J. Flow Chem. 10 (2020) 241–249, https://doi.org/10.1007/s41981-019-00069-2.

[52] M.O. Besenhard, P. Neugebauer, C. Da Ho, J.G. Khinast, Crystal size control in a continuous tubular crystallizer, Cryst. Growth Des. 15 (2015) 1683–1691, https://doi.org/10.1021/cg501637m.

[53] S.V. Savvopoulos, M.N. Hussain, J. Jordens, S. Waldherr, T. Van Gerven, S. Kuhn, A mathematical model of the ultrasound-assisted continuous tubular crystallization of aspirin, Cryst. Growth Des. 19 (2019) 5111–5122, https://doi.org/10.1021/acs.cgd.9b00466.

[54] M.N. Hussain, J. Jordens, J.J. John, L. Braeken, T. Van Gerven, Enhancing pharmaceutical crystallization in a flow crystallizer with ultrasound: anti-solvent crystallization, Ultrason. Sonochem. 59 (2019) 104743 https://doi.org/10.1016/j.ultsonch.2019.104743.

[55] B. Rimez, J. Septavaux, R. Debuysschère, B. Scheid, The creation and testing of a fully continuous tubular crystallization device suited for incorporation into flow chemistry setups, J. Flow Chem. 9 (2019) 237–249, https://doi.org/10.1007/s41981-019-00042-z.

[56] R.J.P. Eder, S. Schrank, M.O. Besenhard, E. Roblegg, H. Gruber-Woelfler, J.G. Khinast, Continuous sonocrystallization of acetylsalicylic acid (ASA): control of crystal size, Cryst. Growth Des. 12 (2012) 4733–4738, https://doi.org/10.1021/cg201567y.

[57] P. Neugebauer, J. Cardona, M.O. Besenhard, A. Peter, H. Gruber-Woelfler, C. Tachtatzis, A. Cleary, I. Andonovic, J. Sefcik, J.G. Khinast, Crystal shape modification via cycles of growth and dissolution in a tubular crystallizer, Cryst. Growth Des. 18 (2018) 4403–4415, https://doi.org/10.1021/acs.cgd.8b00371.

[58] S.V. Savvopoulos, M.N. Hussain, T. Van Gerven, S. Kuhn, Theoretical study of the scalability of a sonicated continuous crystallizer for the production of aspirin, Ind. Eng. Chem. Res. 59 (2020) 19952–19963, https://doi.org/10.1021/acs.iecr.0c03975.

[59] M. Furuta, K. Mukai, D. Cork, K. Mae, Continuous crystallization using a sonicated tubular system for controlling particle size in an API manufacturing process, Chem. Eng. Process. Process Intensif. 102 (2016) 210–218, https://doi.org/10.1016/j.cep.2016.02.002.

[60] C. Ricardo, N. Xiongwei, Evaluation and establishment of a cleaning protocol for the production of vanisal sodium and aspirin using a continuous oscillatory baffled reactor, Org. Process. Res. Dev. 13 (2009) 1080–1087, https://doi.org/10.1021/op900120h.

[61] B. Rimez, J. Septavaux, B. Scheid, The coupling of in-flow reaction with continuous flow seedless tubular crystallization, React. Chem. Eng. 4 (2019) 516–522, https://doi.org/10.1039/C8RE00313K.

[62] K. Tacsi, H. Pataki, A. Domokos, B. Nagy, I. Csontos, I. Markovits, F. Farkas, Z.K. Nagy, G. Marosi, Direct processing of a flow reaction mixture using continuous mixed suspension mixed product removal crystallizer, Cryst. Growth Des. 20 (2020) 4433–4442, https://doi.org/10.1021/acs.cgd.0c00252.

[63] K. Tacsi, A. Joo, E. Pusztai, A. Domokos, Z.K. Nagy, G. Marosi, H. Pataki, Development of a triple impinging jet mixer for continuous antisolvent crystallization of acetylsalicylic acid reaction mixture, Chem. Eng. Process. Process Intensif. (2021) 108446 https://doi.org/10.1016/j.cep.2021.108446.

[64] A. Balogh, A. Domokos, B. Farkas, A. Farkas, Z. Rapi, D. Kiss, Z. Nyiri, Z. Eke, G. Szarka, R. Örkényi, B. Mátravölgyi, F. Faigl, G. Marosi, Z.K. Nagy, Continuous end-to-end production of solid drug dosage forms: coupling flow synthesis and formulation by electrospinning, Chem. Eng. J. 350 (2018) 290–299, https://doi.org/10.1016/j.cej.2018.05.188.

[65] B. Nagy, B. Szilágyi, A. Domokos, B. Vészi, K. Tacsi, Z. Rapi, H. Pataki, G. Marosi, Z.K. Nagy, Z.K. Nagy, Dynamic flowsheet model development and digital design of continuous pharmaceutical manufacturing with dissolution modeling of the final product, Chem. Eng. J. (2021) 129947 https://doi.org/10.1016/j.cej.2021.129947.

[66] N.J. Mozdzierz, Y. Lee, M.S. Hong, M.H.P. Benisch, M.L. Rasche, U.E. Tropp, M. Jiang, A.S. Myerson, R.D. Braatz, Mathematical modeling and experimental validation of continuous slug-flow tubular crystallization with ultrasonication-induced nucleation and spatially varying temperature, Chem. Eng. Res. Des. 169 (2021) 275–287, https://doi.org/10.1016/j.cherd.2021.03.026.

[67] B. Gielen, J. Jordens, L.C.J. Thomassen, L. Braeken, T. Van Gerven, Agglomeration control during ultrasonic crystallization of an active pharmaceutical ingredient, Crystals. 7 (2017) 1–20, https://doi.org/10.3390/cryst7020040.

[68] X. Cheng, X. Huang, B. Tian, T. Wang, H. Hao, Behaviors and physical mechanism of ceftezole sodium de-agglomeration driven by ultrasound, Ultrason. Sonochem. 74 (2021) 105570 https://doi.org/10.1016/j.ultsonch.2021.105570.